



Cite this: *New J. Chem.*, 2021, **45**, 3181

# Functionalized resorcin[4]arene-based coordination polymers as heterogeneous catalysts for click reactions†

Fei-Fei Wang,<sup>‡a</sup> Jia-Hui Li,<sup>‡a</sup> Hai-Yan Liu,<sup>b</sup> Shu-Ping Deng,<sup>b</sup> Ying-Ying Liu<sup>id</sup> <sup>\*a</sup> and Jian-Fang Ma<sup>id</sup> <sup>\*a</sup>

Received 12th December 2020,  
Accepted 13th January 2021

DOI: 10.1039/d0nj06051h

rsc.li/njc

Three distinctive coordination polymers  $[\text{Cu}_2\text{L}_2] \cdot 0.5\text{CH}_3\text{OH} \cdot 1.5\text{H}_2\text{O} \cdot 2\text{CN}$  (**1**),  $[\text{CdCl}_2\text{L}] \cdot 5\text{DMF} \cdot 2\text{CH}_3\text{OH} \cdot 2\text{H}_2\text{O}$  (**2**) and  $[\text{Cd}_2\text{L}(\text{bdc})_2(\text{DMF})] \cdot 2\text{DMF} \cdot 3\text{CH}_3\text{OH} \cdot \text{H}_2\text{O}$  (**3**) were solvothermally synthesized using a resorcin[4]arene ligand ( $\text{H}_2\text{bdc}$  = *p*-phthalic acid and L = tetrakis(4-mercaptopyridine-ylmethyl)resorcin[4]arene). Among them, **1** exhibits a 3D structure, but **2** and **3** are both charming layers. **1** exhibits efficient and selective catalytic performance for azide–alkyne cycloaddition reactions owing to its rich Lewis acid sites. Remarkably, as a heterogeneous catalyst, **1** could be recycled with preservation of the catalytic capability and structural integrity.

## Introduction

The alkyne and azide cycloaddition (AAC) reaction, a “click” reaction is a milestone method in the synthesis of 1,2,3-triazoles.<sup>1–3</sup> Compared with the classical Huisgen azide–alkyne 1,3-dipolar cycloaddition reactions, Cu(I)-based AAC reactions exhibit obvious advantages, like extremely high regioselectivity, mild reaction conditions, easy operation, and high yields.<sup>4–7</sup> Therefore, CuAAC reactions have been widely utilized in organic synthesis,<sup>8,9</sup> medicinal chemistry,<sup>10,11</sup> chemical biology,<sup>12–14</sup> and materials science.<sup>15,16</sup> Focusing on this reaction, a lot of Cu-based catalysts have been developed. CuCl, CuBr and CuSO<sub>4</sub>/reducers are typical homogeneous catalysts.<sup>17,18</sup> But they feature the disadvantage of easy-destruction or difficulty in separating from the reaction system.<sup>19</sup> In order to improve the catalytic efficiency, heterogeneous catalysts, such as Cu(I)-based coordination polymers (CPs), have been developed.<sup>20–27</sup>

Resorcin[4]arene, as a subclass of calix[4]arenes, has unique cavities and various functional moieties.<sup>28–30</sup> Their mainbody and rims could be modified by a number of groups, and these

substituents provide multiple coordination sites when reacting with metal ions.<sup>31–34</sup> Scores of CPs with various structures and properties have been continuously employed based on functional-resorcin[4]arene macrocyclic ligands. As to the catalytic properties of resorcin[4]arene-based CPs, several groups have carried out research on this topic. Pioneering research studies suggest that resorcin[4]arene-based CPs show efficient catalytic performances in epoxidation of olefins,<sup>35</sup> Knoevenagel condensation,<sup>36</sup> oxidation desulfurization,<sup>37</sup> C–H oxidation of fluorene,<sup>38</sup> and click reactions.<sup>39</sup>

In this study, we prepared a functional resorcin[4]arene ligand modified by four 4-mercapto-pyridine groups. Through the assembly of cadmium and copper salts with L,  $[\text{Cu}_2\text{L}_2] \cdot 0.5\text{CH}_3\text{OH} \cdot 1.5\text{H}_2\text{O} \cdot 2\text{CN}$  (**1**),  $[\text{CdCl}_2\text{L}] \cdot 5\text{DMF} \cdot 2\text{CH}_3\text{OH} \cdot 2\text{H}_2\text{O}$  (**2**) and  $[\text{Cd}_2\text{L}(\text{bdc})_2(\text{DMF})] \cdot 2\text{DMF} \cdot 3\text{CH}_3\text{OH} \cdot \text{H}_2\text{O}$  (**3**) have been synthesized successfully. Significantly, **1** exhibits good heterogeneous catalytic capability for AAC reactions in the formation of 1,2,3-triazoles as well as  $\beta$ -OH-1,2,3-triazoles.

## Experimental section

### Synthesis of L

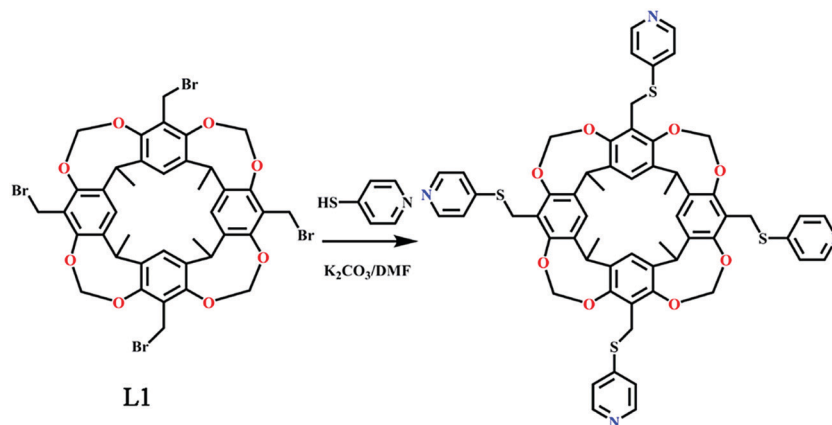
First, we synthesized precursor L1 by using the reported method.<sup>40</sup> L1 (10.0 mmol), anhydrous K<sub>2</sub>CO<sub>3</sub> (100.0 mmol), 4-mercaptopyridine (50.0 mmol) and DMF (200 mL) were added to the flask in turn and heated at 90 °C under N<sub>2</sub> for 10 hours. The reaction was monitored by thin layer chromatography. Then, the obtained solid was suction filtrated, rotary evaporated and washed with water. The crude product was recrystallized using CH<sub>2</sub>Cl<sub>2</sub>–CH<sub>3</sub>OH to obtain light yellow L with a yield of 85% (Scheme 1 and Fig. S1–S3, ESI†).

<sup>a</sup> Key Lab of Polyoxometalate Science, Department of Chemistry, Northeast Normal University, Changchun 130024, China. E-mail: liuyy147@nenu.edu.cn, majf247@nenu.edu.cn

<sup>b</sup> Key Lab of Chemical Additive Synthesis and Separation, Department of Chemical and Environmental Engineering, Yingkou Institute of Technology, Yingkou 115014, China

† Electronic supplementary information (ESI) available. CCDC crystallographic data and structure refinements, PXRD patterns, infrared spectra, TGA curves, selected bond distances and angles of 1–3, GC and <sup>1</sup>H NMR of the AAC reactions are provided. CCDC 2048218–2048220 for 1–3. For ESI and crystallographic data in CIF or other electronic format see DOI: 10.1039/d0nj06051h

‡ These authors contributed equally.



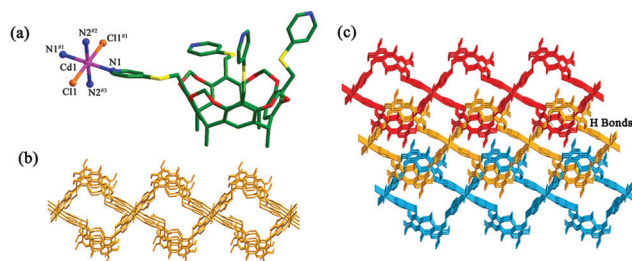
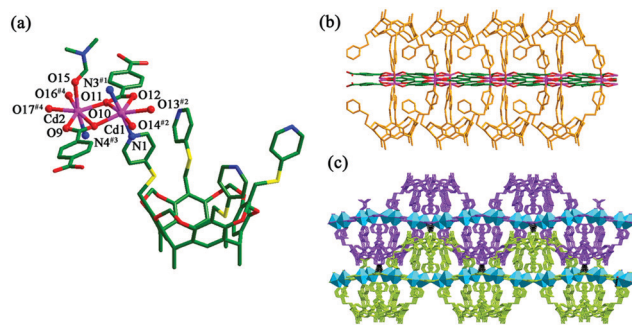
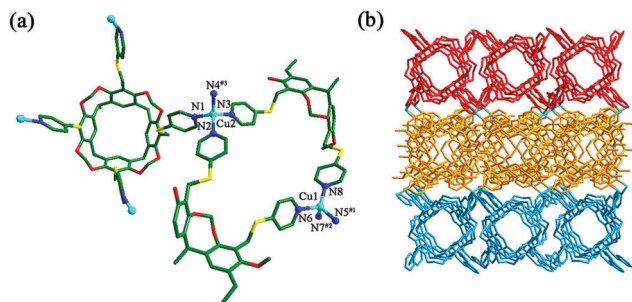
Scheme 1 Schematic synthesis of L.

### Synthesis of $[\text{Cu}_2\text{L}_2] \cdot 0.5\text{CH}_3\text{OH} \cdot 1.5\text{H}_2\text{O} \cdot 2\text{CN}$ (1)

$\text{Cu}(\text{NO}_3)_2 \cdot 2\text{H}_2\text{O}$  (10 mg, 0.04 mmol), L (11 mg, 0.01 mmol), fumaric acid (5 mg, 0.04 mmol) and DMF/methanol V/V = 5/3 were added to a 15 mL vessel and reacted at 100 °C for three days. After cooling, pale green massive crystals were isolated. The yield was calculated to be 53% based on L. Anal. calcd for  $\text{C}_{122.5}\text{H}_{109}\text{N}_{10}\text{O}_{18}\text{S}_8\text{Cu}_2$  ( $M_r = 2390$ ): C, 61.51; H, 4.56; N, 5.86; S, 10.71; found: C, 55.07; H, 4.71; N, 5.83; S, 9.60; IR ( $\text{cm}^{-1}$ ): 3421(w), 2970(w), 2942(w), 2882(w), 1656(w), 1588(s), 1532(w), 1474(m), 1416(m), 1384(m), 1333(m), 1253(m), 1211(w), 1148(w), 1104(s), 1092(m), 1051(w), 1017(m), 977(s), 932(m), 807(m), 754(w), 717(m), 689(w), 646(w), 579(w), 564(w), 493(w) (Fig. S5, ESI†).

### Synthesis of $[\text{CdCl}_2\text{L}] \cdot 5\text{DMF} \cdot 2\text{CH}_3\text{OH} \cdot 2\text{H}_2\text{O}$ (2)

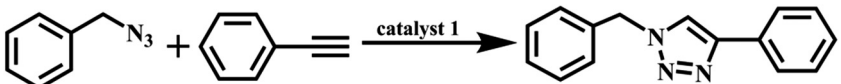
$\text{CdCl}_2 \cdot 2.5\text{H}_2\text{O}$  (10 mg, 0.04 mmol), L (12 mg, 0.01 mmol), proline acid (5 mg, 0.04 mmol) and DMF/methanol (V/V = 3/1) were reacted at 100 °C for three days. After cooling, transparent crystals were obtained (yield = 44%). Anal. calcd for  $\text{C}_{82}\text{H}_{97}\text{N}_9\text{O}_8\text{S}_4\text{Cl}_2\text{Cd}$  ( $M_r = 1732.4$ ): C, 56.79; H, 5.59; N, 7.27; S, 7.38; found: C, 50.61; H, 5.35; N, 6.60; S, 7.65; IR ( $\text{cm}^{-1}$ ): 3430(w), 2967(w), 2938(w), 2877(w), 1662(s), 1581(s), 1458(m), 1421(m), 1379(m), 1338(w), 1301(w), 1249(w), 1220(w), 1146(w), 1092(m), 1047(w), 1006(m), 977(s), 920(m), 809(w), 719(w), 657(w), 584(w), 498(w).

Fig. 2 (a) Coordination environment of Cd1 in **2**. (b) View of the 2D layer. (c) The 3D supramolecular structure constructed via H-bonds.Fig. 3 (a) Coordination environment of Cd1 and Cd2 ions in **3**. (b) View of the 2D layer. (c) The 3D supramolecular structure.Fig. 1 (a) Coordination environments of Cu1 and Cu2 in **1**. (b) The 3D framework.

### Synthesis of $[\text{Cd}_2\text{L}(\text{bdc})_2(\text{DMF})] \cdot 2\text{DMF} \cdot 3\text{CH}_3\text{OH} \cdot \text{H}_2\text{O}$ (3)

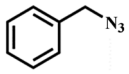
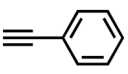
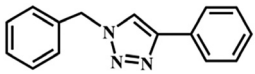
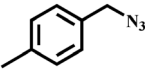
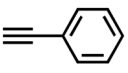
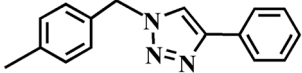
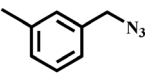
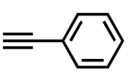
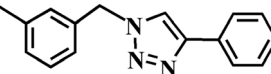
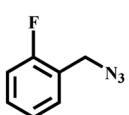
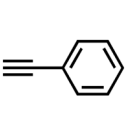
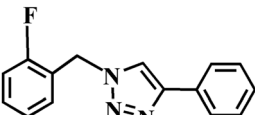
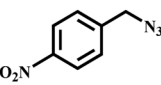
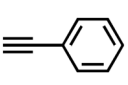
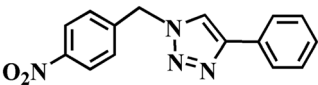
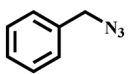
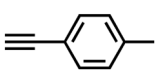
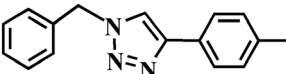
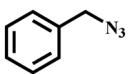
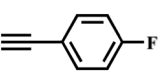
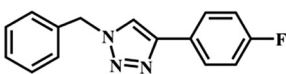
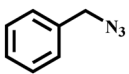
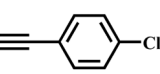
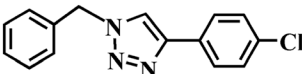
$\text{CdCl}_2 \cdot 2.5\text{H}_2\text{O}$  (10 mg, 0.04 mmol), L (11 mg, 0.01 mmol), *p*-H<sub>2</sub>bdc (7 mg, 0.04 mmol) and DMF/methanol V/V = 6/2 were reacted at 100 °C for three days. Light yellow massive crystals were obtained (yield = 14%). Anal. calcd for  $\text{C}_{103}\text{H}_{115}\text{N}_{10}\text{O}_{28}\text{S}_4\text{Cd}_2$  ( $M_r = 2291$ ): C, 53.95; H, 5.02; N, 6.11; S, 5.58; found: C, 50.18; H, 5.63; N, 5.92; S, 5.49; IR ( $\text{cm}^{-1}$ ): 3430(w), 2933(w), 2270(w), 1661(s), 1591(s), 1556(s), 1502(m), 1469(m), 1385(s), 1250(w), 1227(w), 1147(w), 1094(m), 1051(w), 1013(m), 976(s), 928(w), 842(w), 807(w), 754(m), 720(w), 685(w), 662(w), 581(w), 496(w).

Table 1 The AAC reactions under different conditions

							
Entry	Catalyst (mg)	Time (h)	Temperature (°C)	Solvent	Conversion (%)	TON <sup>a</sup>	TOF <sup>b</sup> (h <sup>-1</sup> )
1	None	5	80	MeOH	13	0	0
2	5	5	80	MeOH	> 99	471	94.2
3	5	5	80	EtOH	96	457	91.4
4	5	5	80	MeCN	27	129	25.8
5	5	5	RT	MeOH	3	14	2.8
6	5	5	40	MeOH	23	110	22.0
7	5	5	60	MeOH	64	61	61.0

<sup>a</sup> Per-mole catalyst for mole product. <sup>b</sup> Per-mole catalyst per-hour for mole product.

Table 2 AAC catalytic reaction with different substituents<sup>a</sup>

Entry	Azide	Alkyne	Product	Conversion (%)	TON	TOF (h <sup>-1</sup> )
1				99	471	94.2
2				99	471	94.2
3				99	471	94.2
4				99	471	94.2
5				99	471	94.2
6				88	419	83.8
7				33	157	31.4
8				56	267	53.4

<sup>a</sup> Reaction conditions: catalyst (5 mg, 0.21% mmol), azide (1 mmol), acetate (0.92 mmol), alkyne (2 mmol) and MeOH (4 mL), 80 °C, 5 h.

## Results and discussion

### Structure of [Cu<sub>2</sub>L<sub>2</sub>]·0.5CH<sub>3</sub>OH·1.5H<sub>2</sub>O·2CN (1)

The independent unit of **1** constitutes two Cu(I) ions, one whole and two half L ligands, one half free CH<sub>3</sub>OH, one and a half free H<sub>2</sub>O and two CN<sup>-</sup> anions (Fig. 1a). The free CN<sup>-</sup> anions came from the disintegration of DMF, which balanced the cationic charges of the structure.<sup>41,42</sup> Both Cu1 and Cu2 are four-coordinated in regular tetrahedral geometries, defined by four L ligands, respectively. Three individual bowl-shaped L ligands extended in two directions, of which two half-occupied L ligands are in horizontal arrangement, and the third one is in

vertical arrangement (Fig. 1b). All the N atoms on the L participate in the coordination. By this method, Cu(I) ions are connected by L ligands to form a noteworthy 3D framework (Fig. 1b).

### Structure of [CdCl<sub>2</sub>L]<sub>2</sub>·5DMF·2CH<sub>3</sub>OH·2H<sub>2</sub>O (2)

The independent unit of **2** contains one Cd(II) ion, one L, two Cl<sup>-</sup> anions, five free DMF, two free CH<sub>3</sub>OH and two free H<sub>2</sub>O molecules. Cd1 is located at an inversion center, and is six-coordinated by four pyridyl N atoms from four L ligands and two Cl<sup>-</sup> anions (Fig. 2a). All N atoms of L ligand participate in

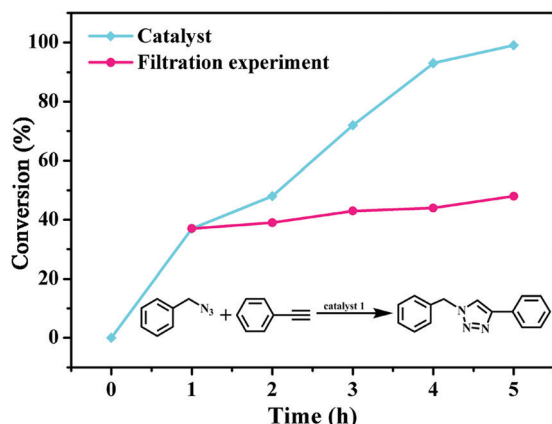


Fig. 4 Kinetic (blue) and hot filtration (pink) experiments catalyzed by **1** for phenylacetylene and benzyl azide reaction.

the coordination, and the ligands link Cd(II) ions to form a charming layered structure (Fig. 2b). The bowl-shaped ligands of each layer are inserted into two adjacent layers, resulting in an interlocked 3D supramolecular structure. Most strikingly, the existence of hydrogen bonds among the interspersed layers further strengthens the 3D supramolecular architecture ( $C12 \cdots O3 = 3.138 \text{ \AA}$ ,  $\angle C12-H12B \cdots O3 = 119.88^\circ$ , Fig. 2c). Calculated by PLATON, the total potential solvent volume occupies about 43.7% of the unit cell ( $2482.4$  and  $5299.4 \text{ \AA}^3$ , respectively).

#### Structure of $[Cd_2L(bdc)_2(DMF)] \cdot 2DMF \cdot 3CH_3OH \cdot H_2O$ (**3**)

There exist two Cd(II) atoms, one ligand, two bdc anions, one coordinated DMF molecule, two free DMF, three free  $CH_3OH$  and one free  $H_2O$  molecule in the asymmetric unit of **3** (Fig. 3a). Both Cd1 and Cd2 are seven-coordinated in pentagonal biconical configurations. Cd1 is surrounded by two N atoms from two L ligands and five O atoms from three bdc anions, whereas the coordination geometry of Cd2 is completed by one N atom from L ligand, six O atoms from three bdc anions and one DMF. The bdc anions connect Cd(II) atoms into a layer. Only three pyridyl N atoms of each L ligand participate in the coordination with Cd(II) ions. L ligands are regularly located

on both sides of the layer (Fig. 3b). Due to the existence of hydrogen bonds ( $C36 \cdots O12 = 3.238 \text{ \AA}$ ,  $\angle C36-H36B \cdots O12 = 123.55^\circ$ ,  $C44 \cdots O10 = 3.300 \text{ \AA}$ ,  $\angle C44-H44 \cdots O10 = 124.11^\circ$ ), the thick layers are further connected to form a fascinating 3D supramolecular structure (Fig. 3c).

#### Catalytic performance of **1** for AAC reactions of benzyl azide

Considering that CP **1** has efficient Lewis acid Cu(I) active sites, **1** was used for catalytic AAC reactions. In the experiment, phenylacetylene and benzyl azide were used as the basic substrates to explore the suitable reaction conditions (Table 1). The conversions were calculated by gas chromatography (Fig. S7, ESI†).

First, the reaction was carried out without adding any catalyst, and a conversion of 13% was achieved (entry 1). Subsequently, to investigate suitable solvents, the catalytic performances were studied in MeCN, EtOH and MeOH. The highest conversion was obtained in MeOH (99%), while the conversions in the other two solvents were 96% and 27%, respectively (entries 2–4). So in the following experiments, MeOH was utilized as the optimal solvent. Next, the experiments were conducted at different temperatures, and lower conversions of 3%, 23% and 64% were obtained at RT,  $40^\circ\text{C}$  and  $60^\circ\text{C}$ , respectively (entries 5–7).

To further determine the general applicability of catalyst **1** to AAC reactions, a series of azides and alkynes with different functional groups were investigated under suitable reaction conditions (Table 2 and Fig. S8, S9–S16, ESI†).

When benzyl azide with 4- $CH_3$ -, 3- $CH_3$ -, 2-F- and 4- $NO_2$  substituents reacted with phenylacetylene respectively, the conversions all could reach 99% (entries 1–5), which demonstrated that **1** has high catalytic efficiency in these reactions no matter whether the substituent is an electron-donating or electron-withdrawing group. But when the benzyl azide reacted with phenylacetylene derivatives, the conversions decreased significantly. When the substituent was 4- $CH_3$ -, the conversion was 88% (entry 6). As for 4-F- and 4-Cl- substituents, the conversions were as low as 33% and 56%, respectively (entries 7 and 8). The results demonstrate that when benzyl azide

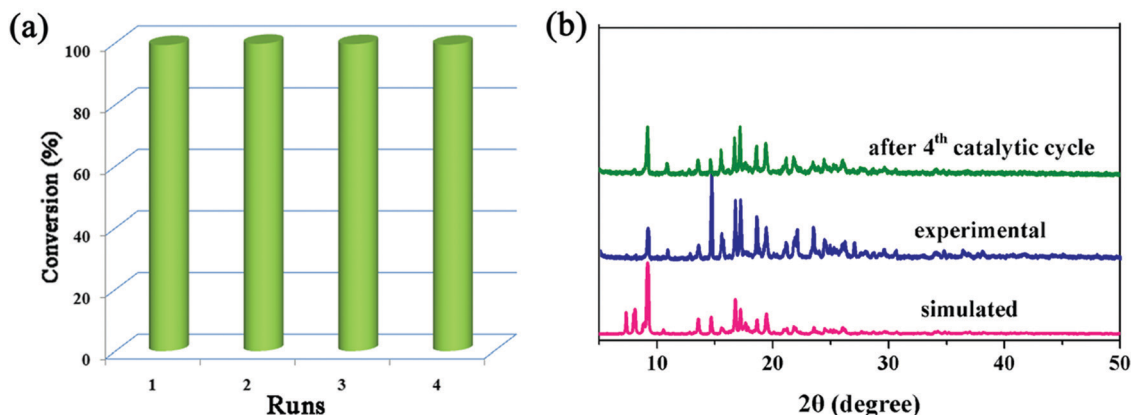


Fig. 5 (a) The conversions of cycling experiments catalyzed by **1** for phenylacetylene and benzyl azide reaction. (b) PXRD patterns of the simulated, the experimental and after the 4th catalytic cycle.

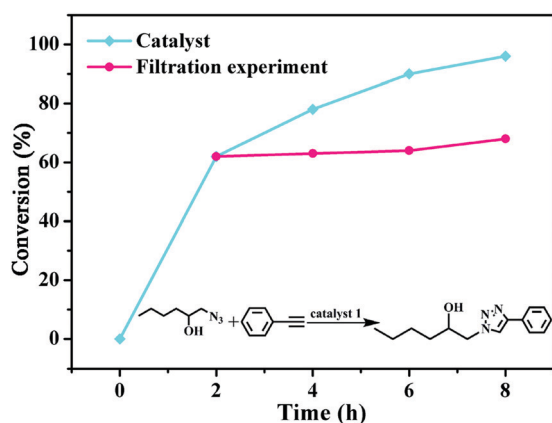
**Table 3** The AAC reactions of phenylacetylene and 1-azido-2-hexanol

Entry	Catalyst (mg)	Time (h)	Temperature (°C)	Solvent	Conversion (%)
1	None	8	80	MeOH	2
2	5	8	80	MeOH	78
3	10	8	80	MeOH	96
4	15	8	80	MeOH	95
5	10	8	80	EtOH	95
6	10	8	80	MeCN	23
7	10	8	RT	MeOH	4
8	10	8	40	MeOH	26
9	10	8	60	MeOH	78

**Table 4** AAC catalytic reaction of different functional groups of  $\beta$ -OH azides with phenylacetylenes<sup>a</sup>

Entry	Alkynes	Azides	Product	Conversion (%)
1				91
2				96
3				99
4				82
5				80

<sup>a</sup> Reaction conditions: catalyst (10 mg, 0.42% mmol),  $\beta$ -OH azide (2 mmol), alkyne (1 mmol), and ethylbenzene (106 mg, 1 mmol) as an internal standard, MeOH (4 mL), 80 °C, 8 h.

**Fig. 6** Kinetic (blue) and hot filtration (pink) experiments catalyzed by **1** for 1-azido-2-hexanol and phenylacetylene reactions.

reacted with phenylacetylene derivatives, an electron-donating group results in higher conversion than an electron-withdrawing group.<sup>43,44</sup>

To study the reaction process, a kinetic test was started and the conversions were monitored every hour. The conversion increased rapidly to 93% within 4 hours. Then, it gradually reached 99% within the next hour. To identify the heterogeneous quality of **1** for the AAC reaction, hot filtration was conducted after the reaction proceeded for 1 hour. The conversion of the remaining filtrate did not increase significantly in the next 4 hours (Fig. 4 and Fig. S17, ESI<sup>†</sup>). Notably, the ICP test demonstrated that no Cu(I) ions were observed in the filtrate. This fully shows that **1** is a heterogeneous catalyst.

Then, cycling experiments were conducted. After four successive runs, the conversions of the reactions did not change and remained at 99% (Fig. 5a and Fig. S18, ESI<sup>†</sup>). After the catalytic reaction, the PXRD curve of the catalyst was almost the same as the simulation one (Fig. 5b).



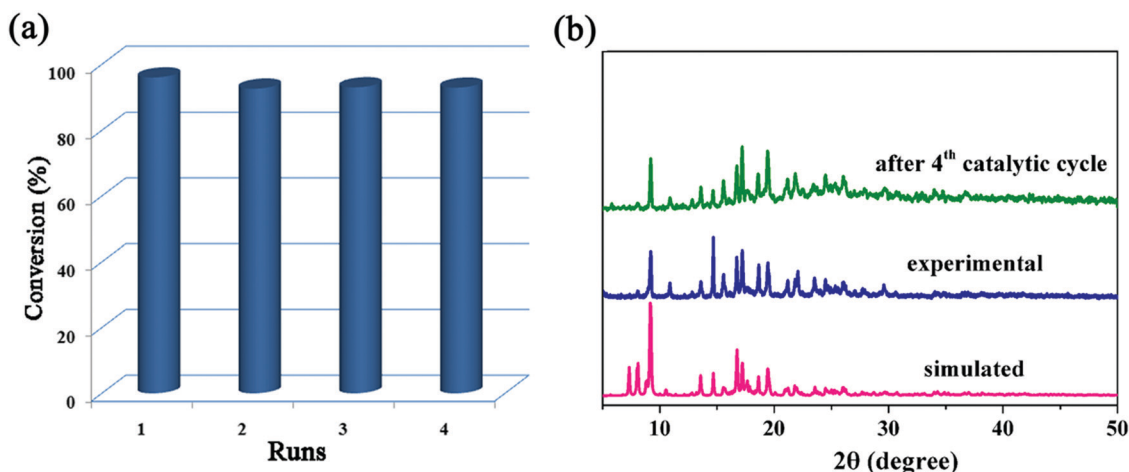


Fig. 7 (a) The conversions of cycling experiments catalyzed by catalyst **1** for 1-azido-2-hexanol and phenylacetylene reaction. (b) PXRD patterns of the simulated, experimental, and after 4th catalytic cycles in 1-azido-2-hexanol and phenylacetylene reaction.

### Catalytic properties of **1** for $\beta$ -OH azide AAC reactions

To date, most CuAAC reactions have been focused on the substrates of alkyl azides or aryl azides, and  $\beta$ -OH-substituted azides have rarely been researched.<sup>45,46</sup> Since **1** exhibits good catalytic activity for phenylacetylene, we further expanded our exploration to other types of substrates, that is  $\beta$ -OH azides. First, phenylacetylene and 1-azido-2-hexanol were utilized as model substrates to study the impact of several parameters (dosage, solvent, temperature and time) on the catalytic reaction (Table 3 and Fig. S19, ESI<sup>†</sup>). Under the conditions of without a catalyst, the conversion was only 2% (entry 1). When **1** was added to the reaction, and the mass of the catalyst was 5, 10 and 15 mg, the conversions were 70%, 96% and 95%, respectively (entries 2–4). So in the follow-up experiment, 10 mg was used as the catalyst dosage. The next reactions were performed in three solvents, MeOH, EtOH and MeCN. A maximal conversion of 96% was obtained in MeOH compared with the other two solvents (entries 5 and 6). By varying the temperature, lower conversions of 4%, 26% and 78% were achieved at RT, 40 °C and 60 °C, respectively (entries 7–9).

To further assess the general usability, we expanded the scope of substrates of catalyst **1** (Table 4 and Fig. S20, S21–S25, ESI<sup>†</sup>). When 4-F-phenylacetylene reacted with 1-azido-2-hexanol, the conversion could reach 91% (entry 1). When phenylacetylene reacted with 1-azido-2-hexanol, 1-azido-2-pentanol, 1-azido-2-butanol and 1-azido-3-phenoxy-2-propanol, the conversions of 96%, 99%, 82% and 80% were obtained, respectively (entries 2–5). The results indicate that **1** exhibits efficient catalytic performance for these reactions.

A kinetic reaction was studied with phenylacetylene and 1-azido-2-hexanol in MeOH at 80 °C. In the first two hours, 62% conversion was rapidly achieved. Then a gradual increase was observed, and reached 96% in the next six hours. To testify the heterogeneity of the reaction, **1** was separated by filtration after 2 hours. Then the reaction went on under the same conditions, and the conversion only has a slight increase of 3% (Fig. 6 and Fig. S26, ESI<sup>†</sup>). ICP data showed that Cu(I) was not observed in the filtrate.

In the following cycling tests, the conversion after four successive runs had only a slight decrease from 96% to 92% (Fig. 7a and Fig. S27, ESI<sup>†</sup>). Remarkably, the PXRD curve of **1** after four catalytic experiments matched well with its original one (Fig. 7b), exhibiting that the structure of **1** did not change. Thus, the recycling experiments further proved the reusability of **1**.

## Conclusions

In summation, one Cu(I) and two Cd(II) CPs were successfully assembled by incorporating a 4-mercaptopyridine-functionalized resorcin[4]arene ligand with metal ions. **1** displays a fascinating 3D structure, and **2** and **3** exhibit layered structures. Strikingly, **1** exhibits an efficient catalytic activity in AAC reactions. It has good stability and could be easily separated from catalytic systems. After cycling, **1** could retain efficiency and its integrity was maintained. The catalytic experiments illustrate that **1** is a splendid heterogeneous catalyst for the synthesis of 1,2,3-triazoles as well as  $\beta$ -OH-1,2,3-triazoles.

## Author contributions

Fei-Fei Wang: Investigation. Jia-Hui Li: Software and writing-original draft. Hai-Yan Liu: Visualization. Shu-Ping Deng: Resources. Ying-Ying Liu: Data curation, validation, and writing – review & editing. Jian-Fang Ma: Conceptualization and funding acquisition.

## Conflicts of interest

There are no conflicts to declare.

## Acknowledgements

This work was supported by the National Natural Science Foundation of Liaoning Province (Grant No. 2019-ZD-0364).

## References

- 1 V. K. Tiwari, B. B. Mishra, K. B. Mishra, N. Mishra, A. S. Singh and X. Chen, *Chem. Rev.*, 2016, **116**, 3086–3240.
- 2 M. Breugst and H.-U. Reissig, *Angew. Chem., Int. Ed.*, 2020, **59**, 12293–12307.
- 3 F. Liu, Y. Chen and K. N. Houk, *Angew. Chem., Int. Ed.*, 2020, **59**, 12412–12416.
- 4 J. E. Hein and V. V. Fokin, *Chem. Soc. Rev.*, 2010, **39**, 1302–1315.
- 5 L. Liang and D. Astruc, *Coord. Chem. Rev.*, 2011, **255**, 2933–2945.
- 6 M. Meldal and C. W. Tornøe, *Chem. Rev.*, 2008, **108**, 2952–3015.
- 7 M. Bagherzadeh, A. Bayrami, R. Kia, M. Amini, L. J. K. Cook and P. R. Raithby, *Inorg. Chim. Acta*, 2017, **466**, 398–404.
- 8 C. Yang, J. P. Flynn and J. Niu, *Angew. Chem., Int. Ed.*, 2018, **57**, 16194–16199.
- 9 M.-C. Giel, C. J. Smedley, E. R. R. Mackie, T. Guo, J. Dong, T. S. Costa and J. E. Moses, *Angew. Chem., Int. Ed.*, 2020, **59**, 1181–1186.
- 10 F. Sun and W.-B. Zhang, *Chin. J. Chem.*, 2020, **38**, 894–896.
- 11 A. Capci, M. M. Lorion, C. Mai, F. Hahn, J. Hodek, C. Wangen, J. Weber, M. Marschall, L. Ackermann and S. B. Tsogoeva, *Chem. – Eur. J.*, 2020, **26**, 12019–12026.
- 12 C. J. Pickens, S. N. Johnson, M. M. Pressnall, M. A. Leon and C. J. Berkland, *Bioconjugate Chem.*, 2018, **29**, 686–701.
- 13 M. Z. C. Hatit, L. F. Reichenbach, J. M. Tobin, F. Vilela, G. A. Burley and A. J. B. Watson, *Nat. Commun.*, 2018, **9**, 4021–4028.
- 14 T. V. Tran, G. Couture and L. H. Do, *Dalton Trans.*, 2019, **48**, 9751–9758.
- 15 Z. Huang, Y. Zhou, Z. Wang, Y. Li, W. Zhang, N. Zhou, Z. Zhang and X. Zhu, *Chin. J. Polym. Sci.*, 2017, **35**, 317–341.
- 16 Y. Patil, G. Zapsas, Y. Gnanou and N. Hadjichristidis, *J. Polym. Sci.*, 2020, **58**, 163–171.
- 17 O. S. Taskin, G. Yilmaz and Y. Yagci, *ACS Macro Lett.*, 2016, **5**, 103–107.
- 18 W. Jiang, J. Yang, Y.-Y. Liu and J.-F. Ma, *Chem. Commun.*, 2016, **52**, 1373–1376.
- 19 A. Correa, L. Cavallo and S. P. Nola, *Chem. – Eur. J.*, 2006, **12**, 7558–7564.
- 20 J. Wen, K. Wu, D. Yang, J. Tian, Z. Huang, A. S. Filatov, A. Lei and X.-M. Lin, *ACS Appl. Mater. Interfaces*, 2018, **10**, 25930–25935.
- 21 X. R. Jia, G. L. Xu, Z. Y. Du and Y. Fu, *Polyhedron*, 2018, **151**, 515–519.
- 22 J. Chai, P. C. Wang, J. Jia, B. Ma, J. Sun, Y. F. Tao, P. Zhang, L. Wang and Y. Fan, *Polyhedron*, 2018, **141**, 369–376.
- 23 M. Aminia, S. Najafia and J. Janczakb, *Inorg. Chim. Acta*, 2018, **482**, 333–339.
- 24 M. Amini, A. Bayrami, M. N. Marashi, A. Arab, A. Ellern and L. K. Woo, *Inorg. Chim. Acta*, 2016, **443**, 22–27.
- 25 C.-C. Cao, C.-X. Chen, Z.-W. Wei, Q.-F. Qiu, N.-X. Zhu, Y.-Y. Xiong, J.-J. Jiang, D. Wang and C.-Y. Su, *J. Am. Chem. Soc.*, 2019, **141**, 2589–2593.
- 26 A. G. Mahmoud, M. F. Guedes da Silva, K. T. Mahmudov and A. J. L. Pombeiro, *Dalton Trans.*, 2019, **48**, 1774–1785.
- 27 X. Guo, C. Huang, H. Yang, Z. Shao, K. Gao, N. Qin, G. Li, J. Wu and H. Hou, *Dalton Trans.*, 2018, **47**, 16895–16901.
- 28 J. Alex, P. McArdle and P. Crowley, *CrystEngComm*, 2020, **22**, 14–17.
- 29 C. R. Pfeiffer, A. Feaster, S. J. Dalgarno and J. L. Atwood, *CrystEngComm*, 2016, **18**, 222–229.
- 30 M. Gabdulkhaev, M. Ziganshin, A. Buzyurov, C. Schick, S. Solovieva, E. Popova, A. Gubaidullin and V. Gorbachuk, *CrystEngComm*, 2020, **22**, 7002–7015.
- 31 I. Ling, A. N. Sobolevc and C. L. Raston, *CrystEngComm*, 2016, **18**, 4929–4937.
- 32 W.-Y. Pei, G. Xu, J. Yang, H. Wu, B. Chen, W. Zhou and J.-F. Ma, *J. Am. Chem. Soc.*, 2017, **139**, 7648–7656.
- 33 X. Zhu, S. Wang, H. Han, X. Hang, W. Xie and W. Liao, *Cryst. Growth Des.*, 2018, **18**, 225–229.
- 34 K. Stefańska, A. Szafraniec, M. Szymański, M. Wierzbicki, A. Szumna and W. Iwanek, *New J. Chem.*, 2019, **43**, 2687–2693.
- 35 T. A. Azemi and M. Vinodh, *RSC Adv.*, 2015, **5**, 88154–88159.
- 36 X. Han, Y.-X. Xu, J. Yang, X. Xu, C.-P. Li and J.-F. Ma, *ACS Appl. Mater. Interfaces*, 2019, **11**, 15591–15597.
- 37 B.-B. Lu, J. Yang, Y.-Y. Liu and J.-F. Ma, *Inorg. Chem.*, 2017, **56**, 11710–11720.
- 38 K. Djernes, O. Moshe, M. Mettry, D. Richards and R. Hooley, *Org. Lett.*, 2012, **14**, 788–791.
- 39 Q. Qin, G.-H. Xu, Y.-Y. Liu and J.-F. Ma, *Appl. Organomet. Chem.*, 2021, e6146.
- 40 L. Wang, T.-T. Guo, J.-C. Ma, Y.-Y. Liu, G.-H. Xu and J.-F. Ma, *ChemistrySelect*, 2019, **4**, 7351–7357.
- 41 J.-F. Li, P. Du, Y.-Y. Liu, G.-H. Xu and J.-F. Ma, *Dalton Trans.*, 2020, **49**, 3715–3722.
- 42 N. Xu, H. Gan, C. Qin, X. Wang and Z. Su, *Angew. Chem., Int. Ed.*, 2019, **58**, 4649–4653.
- 43 W. Wu, J. W. Wang, Y. K. Wang, Y. J. Huang, Y. F. Tan and Z. Q. Weng, *Angew. Chem., Int. Ed.*, 2017, **56**, 10476–10480.
- 44 L.-J. Yue, Y.-Y. Liu, G.-H. Xu and J.-F. Ma, *New J. Chem.*, 2019, **43**, 15871–15878.
- 45 X.-X. Wang, J. Yang, X. Xu and J.-F. Ma, *Chem. – Eur. J.*, 2019, **25**, 1–9.
- 46 J. Li, Y. Ren, C. Qi and H. Jiang, *Dalton Trans.*, 2017, **46**, 7821–7832.